Decoherence of transported spin in multichannel spin-orbit-coupled spintronic devices: Scattering approach to spin-density matrix from the ballistic to the localized regime

Branislav K. Nikolić and Satofumi Souma
Department of Physics and Astronomy, University of Delaware, Newark, Delaware 19716-2570, USA
(Received 27 February 2004; revised manuscript received 3 December 2004; published 26 May 2005)

By viewing current in the detecting lead of a spintronic device as being an ensemble of flowing spins corresponding to a mixed quantum state, where each spin itself is generally described by an improper mixture generated during the transport where it couples to other degrees of freedom due to spin-orbit (SO) interactions or inhomogeneous magnetic fields, we introduce the spin-density operator associated with such current and express it in terms of the spin-resolved Landauer transmission matrix of the device. This formalism, which provides a complete description of coupled spin-charge quantum transport in open finite-size systems attached to external probes, is employed to understand how initially injected pure spin states, comprising fully spin-polarized current, evolve into the mixed ones corresponding to a partially polarized current. We analyze particular routes that diminish spin coherence (signified by decay of the off-diagonal elements of the current spin-density matrix) in two-dimensional-electron-gas-based devices due to the interplay of the Rashba and/or Dresselhaus SO coupling and (i) scattering at the boundaries or lead-wire interface in ballistic semiconductor nanowires; or (ii) spin-independent scattering off static impurities in both weakly and strongly disordered nanowires. The physical interpretation of spin decoherence in the course of multichannel quantum transport in terms of the entanglement of spin to an effectively zero-temperature "environment" composed of open orbital conducting channels offers insight into some of the key challenges for spintronics: controlling decoherence of transported spins and emergence of partially coherent spin states in all-electrical spin manipulation schemes based on the SO interactions in realistic semiconductor structures. In particular, our analysis elucidates why operation of both ballistic and nonballistic spin-field-effect transistors, envisaged to exploit Rashba and Rashba+Dresselhaus SO coupling, respectively, would demand single-channel transport as the only setup ensuring complete suppression of (D'yakonov-Perel'-type) spin decoherence.

DOI: 10.1103/PhysRevB.71.195328 PACS number(s): 72.25.Dc, 03.65.Yz, 85.35.Ds

I. INTRODUCTION

The major goal of recent vigorous efforts in semiconductor spintronics is to create, store, manipulate at a given location, and transport electron spin through a conventional semiconductor environment.[1] The magnetoresistive sensors, brought about by basic research in metal spintronics,[2,3] have given a crucial impetus for advances in information storage technologies. Furthermore, semiconductor-based spintronics[1,4] offer richer avenues for both fundamental studies and applications because of wider possibilities to engineer semiconductor structures by doping and gating.The two principal challenges[4] for semiconductor spintronics are spin injection and coherent spin manipulation.

The current efficiency of conventional spin injection into a semiconductor (Sm) at room temperature (via Ohmic contacts and at the Fermi energy), based on ferromagnetic (FM) metallic sources of spin currents, is much lower than in the case of metal spintronic structures[5] due to the mismatch in the band structure and transport properties of FMs and Sms.[6] Nevertheless, basic transport experiments at low temperatures can evade paramount problems in spin injection into bulk semiconductors by employing diluted magnetic semiconductors[7] or optical injection techniques[8,9] [note that spin injection and detection in a high-mobility two-dimensional electron gas (2DEG) has turned out to be much more demanding[10]]. Also, quantum-coherent spin filters,[11] quantum spin pumps,[12] and mesoscopic generators of pure (i.e., not accompanied by any net charge current) spin Hall current[13] are expected to offer alternative solutions by making possible spin current induction without using any ferromagnetic elements. In addition, quantum-coherent spintronic devices have been proposed[14–16] that could make possible modulation of conventional (unpolarized) charge current injected into a semiconductor with Rashba spin-orbit (SO) interaction by exploiting spin-sensitive quantum interference effects in mesoscopic conductors of multiply connected geometry (such as rings). Thus, even with successful generation of spin currents in semiconductor nanostructures a challenge remains—careful manipulation of transported spins in classical [such as spin-field-effect transistors[17,18] (spin-FETs)] or quantum (such as mobile spin qubits[19]) information processing devices that will not destroy coherent superpositions of quantum states $a|\uparrow\rangle+b|\downarrow\rangle$ necessary for their operation.

The spin-FET proposal[17] epitomizes one of the most influential concepts to emerge in semiconductor spintronics—replacement of cumbersome traditional spin control via externally applied magnetic fields by all-electrical tailoring of spin dynamics via SO interactions. Electric fields can be produced and controlled in far smaller volumes and on far shorter time scales than magnetic fields, thereby offering possibility for efficient local manipulation of spins and smooth integration with conventional high-speed digital electronic circuits. In the envisaged spin-FET device, spin (with polarization vector oriented in the direction of transport) is injected from the source into the Sm wire, it precesses within this nonmagnetic region in a controlled fashion

due to the Rashba type[20] of SO coupling (arising because of the structure inversion asymmetry of heterostructures) that can be tuned by the gate voltage,[21] and finally enters into the drain electrode with a probability that depends on the angle of precession. Thus, such a polarizer-analyzer electrical transport scheme would be able to modulate the fully spin-polarized source-drain charge current.

Inasmuch as coherent spin states can be quite robust in semiconductor quantum wells due to weak coupling of spin to the external environment, they have been successfully transported over hundreds of micrometers at low temperatures.[22] However, since SO interactions couple the spin and momentum of an electron,[23] they can also enable some of the main mechanisms leading to the decay of spin polarization[4,24] when elastic (off lattice imperfections, nonmagnetic impurities, interfaces, and boundaries) or inelastic (off phonons) charge scattering occurs in a 2DEG. For example, in the semiclassical picture, put forth by D'yakonov and Perel' (DP) for an unbounded system with scattering off static impurities (which does not involve instantaneous spin flip),[25] spin gets randomized due to the change of the effective momentum-dependent Rashba magnetic field $\mathbf{B}_R(\mathbf{k})$ (responsible for spin precession) in each scattering event. Thus, the DP spin relaxation[26] will compete with controlled Rashba spin precession, which can impede the operation of devices involving SO couplings. This has prompted recent reexamination of the spin-FET concept toward possibilities for nonballistic modes of operation where spins could remain coherent even in the presence of charge scattering,[18] in contrast to the original proposal of Datta and Das[17] which essentially requires clean one-dimensional wires.

While inelastic processes inevitably drive the spin polarization to zero in the long-time limit,[27] the DP spin relaxation involves only elastic scattering of impurities, which is incapable[28] of dephasing the full electron wave function. Therefore, in the case of quantum transport through a mesoscopic (phase-coherent) SO-coupled Sm region, where the electron is described by a single wave function,[28,29] the coupling between spin polarization and charge currents can be interpreted as stemming from the entanglement of spin and orbital quantum states[30,31] of single electrons injected and detected through electrodes supporting many orbital conducting channels.[31] Within the entangled single-particle wave function, the spin degree of freedom cannot be described by a pure state any more—that is, the spin becomes subjected to decoherence process akin to mechanisms commonly studied when open quantum systems become entangled with a usually large (and dissipative) environment.[32,33] Since present nanofabrication technologies yield quantum wires with more than one open conducting channel at the Fermi energy (including single-wall carbon nanotubes where spin propagates via two channels[34]), it is important to quantify the degree of coherence of spin transported through such structures in the presence of SO coupling.

The loss of coherence[32,33] of transported spins is encoded into the decay of the off-diagonal elements of their density matrix $\hat{\rho}_s$. Recent theoretical pursuits have offered diverse approaches[35–41] which make it possible to follow the quantum dynamics of $\hat{\rho}_s$ in the course of transport, while treating

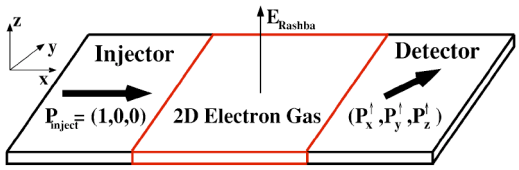

FIG. 1. (Color online) Spin transport through generic two-probe spintronic device where fully spin-polarized current (comprised of pure spin states $|\mathbf{P}|=1$) is injected from the left lead and detected in the right lead. The central region is a 2DEG where the electron can be subjected to a magnetic field and/or SO interactions pertinent to semiconductor heterostructures: Rashba due to the structure inversion asymmetry; and Dresselhaus due to the bulk inversion asymmetry. If the injected current is fully spin polarized, such as along the x axis ($P_x=1, P_y=0, P_z=0$) chosen in the figure, the outgoing current will, in general, have its polarization vector rotated by coherent spin precession in the semiconductor region, as well as shrunk $|\mathbf{P}|<1$ due to processes that lead to loss of spin quantum coherence (such as spin-independent scattering at static impurities or interfaces in the presence of SO coupling).

the ballistic[39,40] or diffusive[35,37,38] propagation of charges (to which the spins are attached) *semiclassically*. The Landauer-Büttiker scattering formalism,[28,29] which intrinsically takes into account phase-coherent propagation of electrons through finite-size devices attached to external current and voltage probes, is also frequently employed to treat quantum spintronic transport in semiconductor structures.[42–46] However, previous applications of the scattering formalism evaluate only the spin-resolved charge conductances which, on the other hand, do not provide enough information to extract the full density matrix of transported spins, "hiding" in the quantum transmission properties of the device. Such approaches yield only a single component of the spin-polarization vector of detected current in the right lead of Fig. 1, while all three components are needed to (i) determine the vector of spin current flowing together with charge current in this lead; (ii) evaluate the density matrix of the corresponding ensemble of transported spins; and (iii) extract their degree of coherence.[32,33,47]

Here we demonstrate how to associate the spin-density matrix with detected current, which emerges after charge current with arbitrary spin-polarization properties (unpolarized, partially polarized, or fully spin-polarized) is injected through multichannel leads and propagated through a quantum-coherent semiconductor nanostructure where transported electrons are subjected to spin-dependent interactions. Following our earlier analysis of the density matrix of a single spin injected through one of the Landauer conducting channels,[31] we introduce in Sec. II a density matrix of an ensemble of spins flowing through the detecting lead in Fig. 1. This central tool of our approach is expressed in terms of both the amplitudes and the phases of (spin-resolved) Landauer transmission matrix elements. In Sec. II B we extract from it the spin-polarization vector $(P_x^{\sigma}, P_y^{\sigma}, P_z^{\sigma})$ of the outgoing current in Fig. 1 while taking into account different possibilities for the polarization σ of the incoming current. This also allows us to elucidate rigorous way of quantifying the spin polarization (as a scalar quantity) of current which is measured in spin detection experiments.[10,23,48] Together with

the Landauer formulas for spin-resolved charge conductances (which involve only the squared amplitudes of the transmission matrix elements[42–46]), our equations for $(P_x^\sigma, P_y^\sigma, P_z^\sigma)$ offer a complete description of the coupled spin-charge quantum transport in finite-size devices where experimentally relevant boundary conditions (such as closed boundaries at which current must vanish, interfaces, external electrodes, and spin-polarization properties of the injected current), which are crucial for the treatment of transport in the presence of SO couplings,[40] are easily incorporated.

The magnitude of **P** quantifies the degree of coherence of the spin state. We employ this formalism in Sec. III to study how spin-orbit entanglement affects transport, entailing the reduction of $|\mathbf{P}|$ in ballistic (Sec. III A) or disordered (Sec. III B) semiconductor multichannel quantum wires. This also offers a direct insight into the dynamics of quantum coherence of spin which would propagate through multichannel ballistic[17] (with Rashba coupling) or nonballistic (with Rashba=Dresselhaus coupling) spin-FET devices.[18] For the transport of noninteracting electrons through finite-size structures, $(P_x^\sigma, P_y^\sigma, P_z^\sigma)$ can be evaluated nonperturbatively in both the SO couplings and the disorder strength. This makes it possible to treat the dynamics of spin coherence in a wide range of transport regimes (from high mobility in ballistic to low mobility in localized systems), thereby unearthing quantum effects in the evolution of $|\mathbf{P}|$ that go beyond conventional semiclassical[25] or perturbative quantum treatments[49] of spin relaxation in diffusive bulk semiconductors with weak SO interaction. We conclude in Sec. IV by highlighting requirements to combat spin decoherence in spintronic devices relying on fully coherent spin states, while also pointing out at capabilities of partially coherent spin states that inevitably emerge in multichannel devices examined here.

II. PURITY OF TRANSPORTED SPIN STATES

For the understanding of quantum dynamics of open spin systems and processes which leak their coherence into the environment,[32,33] the central role is played by the density operator[47,50] $\hat{\rho}_s$. The expectation value $\langle\Sigma|\hat{\rho}_s|\Sigma\rangle$ gives the probability of observing the system in state $|\Sigma\rangle$. For spin-$\frac{1}{2}$ particle, this operator has a simple representation in a chosen basis[50] $|\uparrow\rangle, |\downarrow\rangle \in \mathcal{H}_s$,

$$\hat{\rho}_s = \begin{pmatrix} \rho_{\uparrow\uparrow} & \rho_{\uparrow\downarrow} \\ \rho_{\downarrow\uparrow} & \rho_{\downarrow\downarrow} \end{pmatrix} = \frac{\hat{I}_s + \mathbf{P}\cdot\hat{\boldsymbol{\sigma}}}{2}, \tag{1}$$

which is a 2×2 spin density matrix where $\hat{I}_s$ is the unit operator in the spin Hilbert space and $\hat{\boldsymbol{\sigma}}=(\hat{\sigma}_x,\hat{\sigma}_y,\hat{\sigma}_z)$ is the vector of Pauli spin matrices. The diagonal elements $\rho_{\uparrow\uparrow}$ and $\rho_{\downarrow\downarrow}$ represent the probabilities to find an electron with spin $\uparrow$ or spin $\downarrow$. The off-diagonal elements $\rho_{\uparrow\downarrow}, \rho_{\downarrow\uparrow}$ define the amount by which the probabilities of coherent superpositions of basis vectors $|\uparrow\rangle, |\downarrow\rangle$ deviate, due to quantum-interference effects, from the classical (incoherent) mixture of states. The two-level system density matrix Eq. (1) is the simplest example of its kind since it is determined just by a set of three real numbers representing the components of the spin polarization[47,50] (or Bloch) vector $\mathbf{P}=(P_x,P_y,P_z)$. For spin-$\frac{1}{2}$ particles, the polarization vector is experimentally measured as the quantum-mechanical average

$$\frac{\hbar}{2}\mathbf{P} = \frac{\hbar}{2}(\langle\hat{\sigma}_x\rangle,\langle\hat{\sigma}_y\rangle,\langle\hat{\sigma}_z\rangle) = \mathrm{Tr}\left[\hat{\rho}_s\frac{\hbar}{2}\hat{\boldsymbol{\sigma}}\right], \tag{2}$$

which is the expectation value of the spin operator $\hbar\hat{\boldsymbol{\sigma}}/2$.

A fully coherent state of spin-$\frac{1}{2}$ particle is pure and, therefore, described formally by a vector $|\Sigma\rangle$ belonging to the two-dimensional Hilbert space $|\Sigma\rangle \in H_s$. The density operator formalism encompasses both *pure* $\hat{\rho}=|\Sigma\rangle\langle\Sigma|$ states and *mixtures* $\hat{\rho}=\Sigma_i w_i|\Sigma_i\rangle\langle\Sigma_i|$ describing an ensemble of quantum states appearing with different classical probabilities w_i. One can quantify the degree of coherence of a quantum state[32] by the purity $\mathcal{P}=\mathrm{Tr}\,\hat{\rho}^2$. However, since the density operator $\hat{\rho}_s$ of a spin-$\frac{1}{2}$ particle is determined solely by the polarization vector **P**, all relevant information about its coherence can be obtained from the magnitude $|\mathbf{P}|=\sqrt{P_x^2+P_y^2+P_z^2}$, so that $\mathcal{P}_s=(1+|\mathbf{P}|^2)/2$ (note that in the case of, e.g., a spin-1 particle one has to measure additional five parameters[50] to specify $\hat{\rho}_s$ and its purity).

For fully coherent pure states the polarization vector has unit magnitude $|\mathbf{P}|=1$, while $0\leqslant|\mathbf{P}|<1$ accounts for mixtures. The dynamics of electron spin is affected by external magnetic field, local magnetic fields produced by magnetic impurities and nuclei, and different types of SO couplings. These interactions not only generate quantum-coherent evolution of the carrier spin, but can also induce spin decoherence.[4,32,33] Thus, coherent motion is encoded into the rotation of vector **P**, while the decay of spin coherence is measured by the reduction of its magnitude $|\mathbf{P}|$ below 1. Figure 1 illustrates how these generic features in the dynamics of open two-level systems will manifest for spins in a nonequilibrium steady transport state.

A. Spin-density matrix of detected current

Most of the traditional mesoscopic experiments[51] explore superpositions of orbital states of transported spin-degenerate electrons since inelastic dephasing processes are suppressed in small enough structures ($L\lesssim 1\ \mu$m) at low temperatures ($T\ll 1$ K). This means that electron is described by a single orbital wave function $|\Psi\rangle\in\mathcal{H}_o$ within the conductor.[28,29] When spin-polarized electron is injected into a phase-coherent semiconductor structures where it becomes subjected to interactions with effective magnetic fields, its state will remain pure, but now in the tensor product of the orbital and the spin Hilbert spaces $|\Psi\rangle\in\mathcal{H}_o\otimes\mathcal{H}_s$. Inside the ideal (free from spin and charge interactions) leads attached to the sample, the electron wave function can be expressed as a linear combination of spin-polarized conducting channels $|n\sigma\rangle=|n\rangle\otimes|\sigma\rangle$ at a given Fermi energy. Each channel, being a tensor product of the orbital transverse propagating mode and a spinor, is a separable[47] pure quantum state $\langle\mathbf{r}|n\sigma\rangle^{\pm}=\Phi_n(y)\otimes\exp(\pm ik_n x)\otimes|\sigma\rangle$ specified by a

real wave number $k_n>0$, a transverse mode $\Phi_n(y)$ defined by the quantization of transverse momentum in the leads of a finite cross section, and a spin factor state $|\sigma\rangle$ (we assume that orbital channels $|n\rangle$ are normalized in the usual way to carry a unit current[29]). When injected spin-polarized flux from the left lead of a two-probe device is concentrated in the spin-polarized channel $|\text{in}\rangle \equiv |n\sigma\rangle$, a pure state emerging in the right lead will, in general, be described by the linear combination of the outgoing channels

$$|\text{out}\rangle = \sum_{n'\sigma'} \mathbf{t}_{n'n,\sigma'\sigma}|n'\rangle \otimes |\sigma'\rangle, \tag{3}$$

which is a nonseparable[47] state. This equation introduces the spin-resolved Landauer transmission matrix where $|\mathbf{t}_{n'n,\sigma'\sigma}|^2$ represents the probability for a spin-σ electron incoming from the left lead in the orbital state $|n\rangle$ to appear as a spin-σ' electron in the orbital channel $|n'\rangle$ in the right lead. The matrix elements of $\mathbf{t}$ depend on the Fermi energy E_F at which quantum (i.e., effectively zero temperature) transport takes place. The $\mathbf{t}$ matrix, extended to include the spin degree of freedom and spin-dependent single-particle interactions in quantum transport,[42,43] is a standard tool to obtain the spin-resolved conductances of a two-probe device,

$$\mathbf{G} = \begin{pmatrix} G^{\uparrow\uparrow} & G^{\uparrow\downarrow} \\ G^{\downarrow\uparrow} & G^{\downarrow\downarrow} \end{pmatrix} = \frac{e^2}{h} \sum_{n',n=1}^{M} \begin{pmatrix} |\mathbf{t}_{n'n,\uparrow\uparrow}|^2 & |\mathbf{t}_{n'n,\uparrow\downarrow}|^2 \\ |\mathbf{t}_{n'n,\downarrow\uparrow}|^2 & |\mathbf{t}_{n'n,\downarrow\downarrow}|^2 \end{pmatrix}. \tag{4}$$

Here M is the number of orbital conducting channels (the number of spin-polarized conducting channels is $2M$) determined by the properties of the transverse confining potential in the leads. In the Landauer picture of spatial separation of single-particle coherent and many-body inelastic processes,[52] it is assumed that the sample is attached to huge electron reservoirs with negligible spin-dependent interactions. To simplify the scattering boundary conditions, semi-infinite ideal leads are inserted between the reservoirs (which thermalize electrons and ensure steady-state transport) and the semiconductor region.

Selecting the spin-resolved elements of the $\mathbf{t}$ matrix (see Sec. III) allows one to describe different spin injection and detection transport measurements. That is, the spin-resolved conductances can be interpreted as describing injection, transport, and detection of single spin species in a setup involving spin filters or half-metallic ferromagnetic leads with collinear magnetization directions. For example, $G^{\uparrow\downarrow}$ is the conductance of a setup where spin-$\downarrow$ polarized current is injected and spin-$\uparrow$ polarized current is detected for $\uparrow$ and $\downarrow$ spin defined by the same spin quantization axis. If both spin species are injected from the left lead in equal proportion, as in the experiments with conventional unpolarized current, one resorts to the usual Landauer conductance formula[28,29] $G=G^{\uparrow\uparrow}+G^{\uparrow\downarrow}+G^{\downarrow\uparrow}+G^{\downarrow\downarrow}$.

While the conductance formulas Eq. (4) require one to evaluate only the amplitude of the $\mathbf{t}$-matrix elements, Eq. (3) reveals that both the amplitude and the phase of $\mathbf{t}_{n'n,\sigma'\sigma}$ determine the nonseparable electron state in the outgoing lead. Although the $|\text{out}\rangle$ state Eq. (3) is still a pure one, spin in such a state is entangled with orbital conducting channels, i.e., it cannot be assigned a single spinor wave function as in the case of $|\text{in}\rangle$ state. Obviously, such SO entanglement will be generated whenever the orbital and spin parts
of the Hamiltonian do not commute, as in cases where, e.g., an inhomogeneous magnetic field,[46] random magnetic impurities, or SO interaction term + inhomogeneous spatial potential[53] govern the quantum evolution of the system.

To each of the outgoing pure states of Eq. (3), we associate a density matrix $\hat{\rho}=|\text{out}\rangle\langle\text{out}|$,

$$\hat{\rho}^{n\sigma\to\text{out}} = \frac{1}{Z} \sum_{n'n''\sigma'\sigma''} \mathbf{t}_{n'n,\sigma'\sigma}\mathbf{t}^*_{n''n,\sigma''\sigma}|n'\rangle\langle n''| \otimes |\sigma'\rangle\langle\sigma''|, \tag{5}$$

where Z is a normalization factor ensuring that $\text{Tr}\,\hat{\rho}=1$. After taking the partial trace[33,50] over the orbital degrees of freedom, which amounts to summing all 2×2 block matrices along the diagonal of $\hat{\rho}^{n\to\text{out}}$, we arrive at the density matrix describing the quantum state of the spin in the right lead.[31] For example, when a spin-$\uparrow$ electron is injected in channel $|n\rangle$ from the left lead, the incoming state is $|n\rangle\otimes|\uparrow\rangle$ and the explicit form of the density matrix for the outgoing spin state in the right lead is given by

$$\hat{\rho}_s^{n\uparrow\to\text{out}} = \frac{1}{Z} \sum_{n'=1}^{M} \begin{pmatrix} |\mathbf{t}_{n'n,\uparrow\uparrow}|^2 & \mathbf{t}_{n'n,\uparrow\uparrow}\mathbf{t}^*_{n'n,\downarrow\uparrow} \\ \mathbf{t}^*_{n'n,\downarrow\uparrow}\mathbf{t}_{n'n,\downarrow\uparrow} & |\mathbf{t}_{n'n,\downarrow\uparrow}|^2 \end{pmatrix}. \tag{6}$$

Since the full outgoing state Eq. (3) of an electron is still pure, the reduced density matrix $\hat{\rho}_s^{n\sigma\to\text{out}}$ does not correspond to any real ensemble of quantum states (i.e., it is an improper mixture[32]). On the other hand, the current can be viewed as a real ensemble of electrons injected in different channels, so that we consider spin and charge flow in the right lead to give rise to an ensemble of states described by a proper mixture $\hat{\rho}_c=\Sigma_n\hat{\rho}_s^{n\sigma\to\text{out}}$. Thus, when spin-$\uparrow$ polarized current is injected from the left lead, we obtain for the current spin-density matrix in the right lead

$$\hat{\rho}_c^{\uparrow} = \frac{e^2/h}{G^{\uparrow\uparrow}+G^{\downarrow\uparrow}} \sum_{n',n=1}^{M} \begin{pmatrix} |\mathbf{t}_{n'n,\uparrow\uparrow}|^2 & \mathbf{t}_{n'n,\uparrow\uparrow}\mathbf{t}^*_{n'n,\downarrow\uparrow} \\ \mathbf{t}^*_{n'n,\uparrow\uparrow}\mathbf{t}_{n'n,\downarrow\uparrow} & |\mathbf{t}_{n'n,\downarrow\uparrow}|^2 \end{pmatrix}. \tag{7}$$

By the same token, the spin-density matrix of the detected current, emerging after the injection of spin-$\downarrow$ polarized charge current, is given by

$$\hat{\rho}_c^{\downarrow} = \frac{e^2/h}{G^{\uparrow\downarrow}+G^{\downarrow\downarrow}} \sum_{n',n=1}^{M} \begin{pmatrix} |\mathbf{t}_{n'n,\uparrow\downarrow}|^2 & \mathbf{t}_{n'n,\uparrow\downarrow}\mathbf{t}^*_{n'n,\downarrow\downarrow} \\ \mathbf{t}^*_{n'n,\uparrow\downarrow}\mathbf{t}_{n'n,\downarrow\downarrow} & |\mathbf{t}_{n'n,\downarrow\downarrow}|^2 \end{pmatrix}. \tag{8}$$

The most general case is obtained after the injection of partially spin-polarized current, whose spins are in the mixed quantum state

$$\hat{\rho}_s = n_\uparrow|\uparrow\rangle\langle\uparrow| + n_\downarrow|\downarrow\rangle\langle\downarrow|, \tag{9}$$

which gives rise to the following spin-density matrix of the outgoing current:

$$\hat{\rho}_c^{\uparrow+\downarrow} = \frac{e^2/h}{n_\uparrow(G^{\uparrow\uparrow}+G^{\downarrow\uparrow})+n_\downarrow(G^{\uparrow\downarrow}+G^{\downarrow\downarrow})} \sum_{n',n=1}^{M} \begin{pmatrix} n_\uparrow|\mathbf{t}_{n'n,\uparrow\uparrow}|^2+n_\downarrow|\mathbf{t}_{n'n,\uparrow\downarrow}|^2 & n_\uparrow \mathbf{t}_{n'n,\uparrow\uparrow}\mathbf{t}^*_{n'n,\downarrow\uparrow}+n_\downarrow \mathbf{t}_{n'n,\uparrow\downarrow}\mathbf{t}^*_{n'n,\downarrow\downarrow} \\ n_\uparrow \mathbf{t}^*_{n'n,\uparrow\uparrow}\mathbf{t}_{n'n,\downarrow\uparrow}+n_\downarrow \mathbf{t}^*_{n'n,\uparrow\downarrow}\mathbf{t}_{n'n,\downarrow\downarrow} & n_\uparrow|\mathbf{t}_{n'n,\downarrow\uparrow}|^2+n_\downarrow|\mathbf{t}_{n'n,\downarrow\downarrow}|^2 \end{pmatrix}. \quad (10)$$

This density matrix reduces to Eq. (7) or Eq. (8) in the limits $n_\uparrow=1$, $n_\downarrow=0$ or $n_\uparrow=0$, $n_\downarrow=1$, respectively.

The measurement of any observable quantity O_s on the spin subsystem within the right lead is described by the reduced spin-density matrix $\langle O_s\rangle=\mathrm{Tr}_s[\hat{\rho}_c\hat{O}_s]$, where $\hat{O}_s$ is a Hermitian operator acting solely in $\mathcal{H}_s$. An example of such measurement is the spin operator itself in Eq. (2). In the case of semiconductor quantum wires explored in Secs. III A and III B, the spin-density matrices in Eqs. (7)–(10) are determined by the polarization of injected current, number of orbital conducting channels in the leads, and spin- and charge-dependent interactions within the wire. They characterize transported electron spin in an open quantum system, and can be easily generalized to multiprobe geometry for samples attached to more than two leads.

B. Spin polarization of charge currents in semiconductor spintronics

What is the spin polarization of current flowing through a spintronic device? In many metal and insulator spintronic structures,[3,5] as well as in some of the semiconductor ones,[12] spin-up $I^\uparrow$ and spin-down currents $I^\downarrow$ comprising charge current $I=I^\uparrow+I^\downarrow$ are independent of each other and the spin quantization axis is usually well defined by external magnetic fields. Therefore, spin polarization is easily quantified by a single number[2,3,5]

$$P=\frac{I^\uparrow-I^\downarrow}{I^\uparrow+I^\downarrow}=\frac{G^{\uparrow\uparrow}-G^{\downarrow\downarrow}}{G^{\uparrow\uparrow}+G^{\downarrow\downarrow}}. \quad (11)$$

Using the language of spin-density matrices, a partially polarized current $P\neq 0$ is an incoherent statistical mixture of $|\uparrow\rangle$ and $|\downarrow\rangle$ states described by Eq. (9) (for $n_\uparrow=n_\downarrow$ we get the conventional completely unpolarized charge current $\hat{\rho}_s=\hat{I}_s/2\Rightarrow|\mathbf{P}|=0$).

Surprisingly enough, quite a few apparently different quantities have been proposed in recent spintronic literature to quantify the spin polarization of detected current in semiconductor devices.[44,46,54,55] In semiconductors with SO coupling, or a spatially dependent interaction with surrounding spins and external inhomogeneous magnetic fields,[46] a nonzero off-diagonal spin-resolved conductance $G^{\uparrow\downarrow}\neq 0\neq G^{\downarrow\uparrow}$ will emerge due to spin precession or instantaneous spin-flip processes. Thus, in contrast to Eq. (11), these expressions[44,46,54,55] for "spin polarization" involve all four spin-resolved conductances defined by Eq. (4). However, they effectively evaluate just one component of the spin-polarization vector along the spin quantization axis (which is usually fixed by the direction of magnetization of ferromagnetic elements or axis of spin filter which specify the orientation of injected spins in Fig. 1). For example, standard applications of the Landauer-Büttiker scattering formalism to ballistic[45] or diffusive transport in a 2DEG with Rashba SO interaction,[44] where only spin-resolved charge conductances are evaluated through Eq. (4), allows one to obtain only $P_x^\uparrow$ in the right lead in Fig. 1. The knowledge of $P_x^\uparrow$ alone is insufficient to quantify the quantum coherence properties of detected spins. Also, in the case of transport of fully coherent spins, where $|\mathbf{P}|=1$ in the right lead, we need to know all three components of the outgoing polarization vector to understand different transformations that the device can perform on the incoming spin.[15,16,19]

Our formalism provides a direct algorithm to obtain the explicit formulas for $(P_x^\sigma,P_y^\sigma,P_z^\sigma)$ from the spin-density matrix Eq. (10) by evaluating the expectation value of the spin operator in Eq. (2). When injected current through the left lead is spin-$\uparrow$ polarized, the spin-polarization vector of the current in the right lead is obtained from Eqs. (2) and (7) as

$$P_x^\uparrow=\frac{G^{\uparrow\uparrow}-G^{\downarrow\uparrow}}{G^{\uparrow\uparrow}+G^{\downarrow\uparrow}}, \quad (12a)$$

$$P_y^\uparrow=\frac{2e^2/h}{G^{\uparrow\uparrow}+G^{\downarrow\uparrow}}\sum_{n',n=1}^{M}\mathrm{Re}[\mathbf{t}_{n'n,\uparrow\uparrow}\mathbf{t}^*_{n'n,\downarrow\uparrow}], \quad (12b)$$

$$P_z^\uparrow=\frac{2e^2/h}{G^{\uparrow\uparrow}+G^{\downarrow\uparrow}}\sum_{n',n=1}^{M}\mathrm{Im}[\mathbf{t}^*_{n'n,\uparrow\uparrow}\mathbf{t}_{n'n,\downarrow\uparrow}]. \quad (12c)$$

Here, and in the formulas below, the x axis is chosen arbitrarily as the spin quantization axis (Fig. 1), $\hat{\sigma}_x|\uparrow\rangle=+|\uparrow\rangle$ and $\hat{\sigma}_x|\downarrow\rangle=-|\downarrow\rangle$, so that Pauli spin algebra has the following representation:

$$\hat{\sigma}_x=\begin{pmatrix}1&0\\0&-1\end{pmatrix},\quad \hat{\sigma}_y=\begin{pmatrix}0&1\\1&0\end{pmatrix},\quad \hat{\sigma}_z=\begin{pmatrix}0&-i\\i&0\end{pmatrix}. \quad (13)$$

Analogously, if the injected current is 100% spin-$\downarrow$ polarized along the x axis we get

$$P_x^\downarrow=\frac{G^{\uparrow\downarrow}-G^{\downarrow\downarrow}}{G^{\uparrow\downarrow}+G^{\downarrow\downarrow}}, \quad (14a)$$

$$P_y^\downarrow=\frac{2e^2/h}{G^{\uparrow\downarrow}+G^{\downarrow\downarrow}}\sum_{n',n=1}^{M}\mathrm{Re}[\mathbf{t}_{n'n,\uparrow\downarrow}\mathbf{t}^*_{n'n,\downarrow\downarrow}], \quad (14b)$$

$$P_z^{\downarrow} = \frac{2e^2/h}{G^{\uparrow\downarrow} + G^{\downarrow\downarrow}} \sum_{n',n=1}^{M} \mathrm{Im}[\mathbf{t}^*_{n'n,\uparrow\downarrow}\mathbf{t}_{n'n,\downarrow\downarrow}]. \tag{14c}$$

Finally, if we impose the unpolarized current $n_\uparrow = n_\downarrow$ as the boundary condition in the left lead, the polarization vector of detected current in the right lead is given by

$$P_x^{\uparrow+\downarrow} = \frac{G^{\uparrow\uparrow} + G^{\uparrow\downarrow} - G^{\downarrow\uparrow} - G^{\downarrow\downarrow}}{G^{\uparrow\uparrow} + G^{\uparrow\downarrow} + G^{\downarrow\uparrow} + G^{\downarrow\downarrow}}, \tag{15a}$$

$$P_y^{\uparrow+\downarrow} = \frac{2e^2}{h} \frac{1}{G^{\uparrow\uparrow} + G^{\uparrow\downarrow} + G^{\downarrow\uparrow} + G^{\downarrow\downarrow}} \sum_{n',n=1}^{M} \mathrm{Re}[\mathbf{t}_{n'n,\uparrow\uparrow}\mathbf{t}^*_{n'n,\downarrow\uparrow} + \mathbf{t}_{n'n,\uparrow\downarrow}\mathbf{t}^*_{n'n,\downarrow\downarrow}], \tag{15b}$$

$$P_z^{\uparrow+\downarrow} = \frac{2e^2}{h} \frac{1}{G^{\uparrow\uparrow} + G^{\uparrow\downarrow} + G^{\downarrow\uparrow} + G^{\downarrow\downarrow}} \sum_{n',n=1}^{M} \mathrm{Im}[\mathbf{t}^*_{n'n,\uparrow\uparrow}\mathbf{t}_{n'n,\downarrow\uparrow} + \mathbf{t}^*_{n'n,\uparrow\downarrow}\mathbf{t}_{n'n,\downarrow\downarrow}]. \tag{15c}$$

Introducing electric[14,17] or magnetic fields[46] to manipulate spin in spintronic devices selects a preferred direction in space, thereby breaking rotational invariance. Thus, as demonstrated in Secs. III A and III B, spin-resolved conductances and components of the polarization vector of the current will depend on the direction of spin in the incoming current with respect to the direction of these fields. In the case of unpolarized injected current, all results are invariant with respect to the rotation of incoming spin since $\hat{\rho}_s = \hat{I}_s/2$ independently of the spin quantization axis. To accommodate different polarizations of incoming current, one has to change the direction of spin quantization axis. This amounts to changing the representation of Pauli matrices Eq. (13) when computing both (i) the transmission matrix, and (ii) the polarization vector from Eq. (2).

While the form of the spin-density matrices, the diagonal Pauli matrix, and the component of spin-polarization vector P_x^σ along the spin quantization axis are unique, the explicit expressions for P_y^σ and P_z^σ depend on the particular form of the chosen representation for the nondiagonal Pauli matrices. The component along the spin quantization axis [P_x^σ in Eq. (15a)] has a simple physical interpretation—it represents normalized difference of the charge currents of spin-$\uparrow$ ($I^\uparrow = G^{\uparrow\uparrow} + G^{\uparrow\downarrow}$) and spin-$\downarrow$ ($I^\downarrow = G^{\downarrow\downarrow} + G^{\downarrow\uparrow}$) electrons flowing through the right lead. The fact that our expression is able to reproduce the commonly used Eq. (11) as a special case demonstrates that the density matrix of transported spin Eq. (10) derived in Sec. II A yields rigorously defined and unequivocal[56] measure of spin polarization. Therefore, in the rest of the paper we reserve the term *spin polarization of charge current*[37,50] for $|\mathbf{P}|$. It is insightful to point out that the same spin-density matrix Eq. (11) also allows us to obtain the vector of spin current[13] $I^s = (\hbar/2e)(I^\uparrow - I^\downarrow)$, $(I_x^s, I_y^s, I_z^s) = (\hbar/2e)(P_x^\sigma I, P_y^\sigma I, P_y^\sigma I)$, flowing together with charge current $I = I^\uparrow + I^\downarrow = GV$ in the right lead of the device in Fig. 1 (biased by the voltage difference V between the leads).

The explicit expressions for the density matrices of detected current $\hat{\rho}_c^\uparrow$, $\hat{\rho}_c^\downarrow$, $\hat{\rho}_c^{\uparrow+\downarrow}$, i.e., the corresponding polarization vectors extracted in Eqs. (12)–(15), together with the Landauer formula for charge conductances Eq. (4), provide a unified description of coupled spin-charge transport in finite-size devices attached to external probes. For such structures, the system size and interfaces through which electrons can enter or leave the device play an essential role in determining their transport properties. The proper boundary conditions, which require considerable effort in theoretical formalisms tailored for infinite systems,[35] are intrinsically taken into account by the Landauer-Büttiker scattering approach to quantum transport. Moreover, the unified description is indispensable for transport experiments which often detect spin current through induced voltages on spin-selective ferromagnetic[5,10,23] or nonferromagnetic probes.[48] The main concepts introduced here are general enough to explain also spin polarization in experiments where spins are detected in optical schemes which observe the polarization of emitted light in electroluminescence processes.[7]

III. SPIN COHERENCE IN TRANSPORT THROUGH MULTICHANNEL SEMICONDUCTOR NANOWIRES

Traditional semiclassical approaches to spin transport[24,25] have been focused on spin diffusion[57] in disordered systems, where SO interaction effects on transport are usually taken into account only through their role in the relaxation of a nonequilibrium spin polarizations. On the other hand, quantum transport theories have been extensively developed to understand the weak-localization-type corrections that SO interactions induce on the charge conduction properties.[53,58,59] Many electrically controlled (via SO couplings) spintronic devices necessitate a mode of operation with ballistically propagating spin-polarized electrons (such as the original spin-FET proposal[17]) in order to retain a high degree of spin coherence. The study of spin relaxation dynamics in ballistic finite-size structures (such as regular or chaotic SO coupled quantum dots[40]) requires techniques that differ from those applied to, e.g., the D'yakonov-Perel' type of spin relaxation in disordered systems with SO interaction (the DP mechanism dominates spin relaxation at low temperatures in bulk samples and quantum wells of III-V semiconductors). Yet another transport regime that requires special treatment occurs in low-mobility systems whose charge propagation is impeded by Anderson localization effects or strong electron-phonon interactions.[60]

To quantify the degree of coherence of transported spin states in a vast range of transport regimes, we provide in this section one possible implementation of the scattering formalism for the spin-density matrix (Sec. II A), which takes as input a microscopic Hamiltonian. This will allow us to trace the dynamics of the spin-polarization vector of current obtained after the injected pure spin quantum state propagate through ballistic, quasiballistic, diffusive, and strongly disordered multichannel semiconductor nanowires with the Rashba and/or the Dresselhaus SO couplings.

The computation of the Landauer transmission matrix $\mathbf{t}$ usually proceeds either phenomenologically, by replacing the

device with an equivalent structure described by a random scattering matrix (which is applicable to specific geometries that must involve disorder or classical chaos due to the boundary scattering,[29] and extendable to include the SO interactions[61]) or by using Hamiltonian formalisms. We model semiconductor heterostructure containing a 2DEG in the xy plane by an effective mass single-particle Hamiltonian with relevant SO interaction terms,

$$\hat{H} = \frac{\hat{p}_x^2 + \hat{p}_y^2}{2m^*} + V_{\text{conf}}(x,y) + V_{\text{disorder}}(x,y) + \frac{\alpha}{\hbar}(\hat{p}_y\hat{\sigma}_x - \hat{p}_x\hat{\sigma}_y) + \frac{\beta}{\hbar}(\hat{p}_x\hat{\sigma}_x - \hat{p}_y\hat{\sigma}_y), \tag{16}$$

where m^* is the effective mass of an electron in a semiconductor heterostructure.[62] Here $V_{\text{conf}}(x,y)$ represents the hard-wall boundary conditions at those device edges through which the current cannot flow. The random potential $V_{\text{disorder}}(x,y)$ is zero for ballistic wires in Sec. III A, and it simulates spin-independent scattering off impurities in Sec. III B. In semiconductor-based devices there are two main contributions to the SO interactions: (a) electrons confined to the 2DEG within semiconductor heterostructures experience strong Rashba SO coupling [third term in Eq. (16)] because of structure inversion asymmetry due to confining potential and differing band discontinuities at the quantum well interface;[20] linear-in-momentum Dresselhaus SO coupling [fourth term in Eq. (16)] which arises in semiconductors with no bulk inversion symmetry (we neglect here the cubic Dresselhaus term).[63] In a GaAs quantum well the two terms are of the same order of magnitude, while the Rashba SO coupling dominates in narrow-band-gap InAs-based structures (the relative strength α/β has recently been extracted from photocurrent measurements[64]).

Although it is possible to evaluate the transmission matrix elements of simple systems (such as single-[14,15] or two-channel structures[55]) described by the Hamiltonian Eq. (16) by finding the stationary states across the lead+sample systems via matching of eigenfunctions in different regions,[15,18,55,65] for efficient modeling of multichannel transport in arbitrary device geometry, as well as to include effects of disorder, it is necessary to switch to some type of single-particle Green function technique.[28] We employ here the real $\otimes$ spin space Green operators, whose evaluation requires one to rewrite the Hamiltonian Eq. (16) in the local orbital basis

$$\hat{H} = \left(\sum_{\mathbf{m}} \varepsilon_{\mathbf{m}} |\mathbf{m}\rangle\langle\mathbf{m}| - t_o \sum_{\langle \mathbf{m},\mathbf{m}' \rangle} |\mathbf{m}\rangle\langle\mathbf{m}'| \right) \otimes \hat{I}_s + \frac{\alpha}{\hbar}(\hat{p}_y \otimes \hat{\sigma}_x - \hat{p}_x \otimes \hat{\sigma}_y) + \frac{\beta}{\hbar}(\hat{p}_x \otimes \hat{\sigma}_x - \hat{p}_y \otimes \hat{\sigma}_y) \tag{17}$$

defined on the $M \times L$ lattice, where L is the length of the wire in units of the lattice spacing a (of the order of a few nanometers when interpreted in terms of the parameters of semiconductor heterostructures employed in experiments[62]), and M is the width of the wire. In 2D systems, M is also the maximum number of conducting channels that can be opened up by positioning E_F in the band center of the Hamiltonian Eq. (17). Here $t_o = \hbar^2/(2m^*a^2)$ is the nearest-neighbor hopping between s orbitals $\langle \mathbf{r}|\mathbf{m}\rangle = \psi(\mathbf{r}-\mathbf{m})$ on adjacent atoms located at sites $\mathbf{m} = (m_x, m_y)$ of the lattice. In the ballistic wires of Sec. III A we set the on-site potential energy $\varepsilon_{\mathbf{m}} = 0$, while the disorder in Sec. III B is simulated via the uniform random variable $\varepsilon_{\mathbf{m}} \in [-W/2, W/2]$. In Eq. (17) $\otimes$ stands for the Kronecker product of matrices, which is the matrix representation of the tensor product of corresponding operators. The tight-binding representation of the momentum operator is given by the matrix $\langle \mathbf{m}|\hat{p}_x|\mathbf{m}'\rangle = \delta_{m_x', m_x \pm 1} i\hbar(m_x - m_x')/2a^2$. Therefore, the matrix elements of the SO terms in Eq. (17) contain spin-orbit hopping parameters $t_{\text{SO}}^R = \alpha/2a$ and $t_{\text{SO}}^D = \beta/2a$, which determine the Rashba and the Dresselhaus SO-coupling-induced spin splitting of the energy bands,[42] respectively. All parameters in the Hamiltonian with the dimension of energy (W, E_F, t_{SO}^R, and t_{SO}^D) will be expressed in the figures in units of standard (orbital) hopping $t_o = 1$ of tight-binding Hamiltonians.

The SO coupling sets the spin precession length $L_{\text{SO}} = \pi/2k_{\text{SO}}$ defined as the characteristic length scale over which spin precesses by an angle π (i.e., the state $|\uparrow\rangle$ evolves into $|\downarrow\rangle$). For example, in the case of the Rashba SO coupling[42] $k_{\text{SO}} = m^*\alpha/\hbar^2$ ($2k_{\text{SO}}$ is the difference of Fermi wave vectors for the spin-split transverse energy subbands of a quantum wire) and[17] $L_{\text{SO}} = \pi t_o a/2t_{\text{SO}}^R$. The spin precession length determines evolution of spin polarization in the course of semiclassical spatial propagation through both the ballistic[40] and the diffusive[25] SO coupled structures (which are sufficiently wide and weakly disordered; see Sec. III B).

The spin-resolved transmission matrix elements

$$\mathbf{t} = 2\sqrt{-\operatorname{Im}\hat{\Sigma}_L^r \otimes \hat{I}_s} \cdot \hat{G}_{1N}^r \cdot \sqrt{-\operatorname{Im}\hat{\Sigma}_R^r \otimes \hat{I}_s},$$

$$\mathbf{t}_{n'n,\uparrow\uparrow} \equiv \mathbf{t}_{2(n'-1)+1,2(n-1)+1},$$

$$\mathbf{t}_{n'n,\uparrow\downarrow} \equiv \mathbf{t}_{2(n'-1)+1,2n},$$

$$\mathbf{t}_{n'n,\downarrow\uparrow} \equiv \mathbf{t}_{2n',2(n-1)+1},$$

$$\mathbf{t}_{n'n,\downarrow\downarrow} \equiv \mathbf{t}_{2n',2n}, \tag{18}$$

are obtained from the Green operator,

$$\hat{G}^r = \frac{1}{E\hat{I}_o \otimes \hat{I}_s - \hat{H} - \begin{pmatrix} \hat{\Sigma}_\uparrow^r & 0 \\ 0 & \hat{\Sigma}_\downarrow^r \end{pmatrix}}, \tag{19}$$

where $\hat{G}_{1L}^r$ is the $2M \times 2M$ submatrix of the Green function matrix $\hat{G}_{\mathbf{mm}',\sigma\sigma'}^r = \langle \mathbf{m},\sigma|\hat{G}^r|\mathbf{m}',\sigma'\rangle$ connecting the layers 1 and L along the direction of transport (the x axis in Fig. 1). The Green function elements yield the probability amplitude for an electron to propagate between two arbitrary sites (with or without flipping its spin during the motion) inside an open conductor in the absence of inelastic processes. Here the self-energies (r, retarded; a, advanced) $\hat{\Sigma}_{L,R}^a = [\hat{\Sigma}_{L,R}^r]^\dagger$,

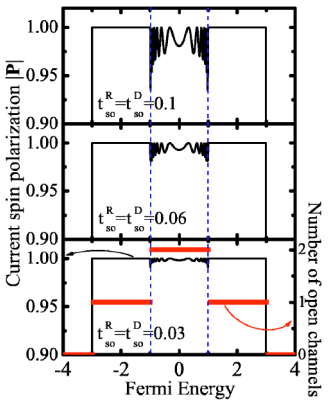

FIG. 2. (Color online) The degree of quantum coherence retained in spins that have been transmitted through a clean two-channel semiconductor nanowire, modeled on the lattice 2×100 by Hamiltonian Eq. (17), for different strengths of the Rashba and the Dresselhaus SO coupling tuned to $t^R_{\rm SO}=t^D_{\rm SO}$. The vertical dashed lines label the position of the Fermi energy in the leads at which the second (orbital) conducting channel becomes available for injection and quantum transport.

$\hat{\Sigma}^r=\hat{\Sigma}^r_L+\hat{\Sigma}^r_R$ account for the "interaction" of the open system with the left (L) or the right (R) lead.[28] For simplicity, we assume that $\hat{\Sigma}^r_\uparrow=\hat{\Sigma}^r_\downarrow$, which experimentally corresponds to identical conditions for the injection of both spin species (as realized by, e.g., two identical half-metallic ferromagnetic leads of opposite magnetization attached to the sample[42]).

A. Ballistic spin-charge quantum transport in semiconductor nanowires with SO interactions

Over the past two decades, a multitude of techniques has been developed to fabricate few nanometer-wide quantum wires and explore their properties in mesoscopic transport experiments. An example is a gated two-dimensional electron gas,[67] which has also become an important component of hybrid spintronic devices.[17] Nevertheless, even for present nanofabrication technology it is still a challenge to fabricate narrow enough wires that can accommodate only one transverse propagating mode.

To investigate spin coherence in multichannel wires, we commence with the simplest example—Fig. 2 plots $|\mathbf{P}|$ as a function of the Fermi energy E_F of electrons whose transmission matrix $\mathbf{t}(E_F)$ determines spin-charge transport in a quantum wire supporting at most two $(n=1,2)$ orbital conducting channels. The current injected from the left lead is assumed to be fully polarized along the direction of transport, as in the case of the spin-FET proposal where such a setup ensures a high level of current modulation.[45] As long as only one conducting channel is open, spin is coherent since the outgoing state in the right lead must be of the form $(a|\uparrow\rangle+b|\downarrow\rangle)\otimes|n=1\rangle$. At exactly the same Fermi energy where the second conducting channel becomes available for quantum transport, the spin polarization drops below 1 and the spin state, therefore, loses its purity $|\mathbf{P}|<1$. This can be explained by the fact that at this E_F, the quantum state of transported spin of an electron in the right lead appears to be

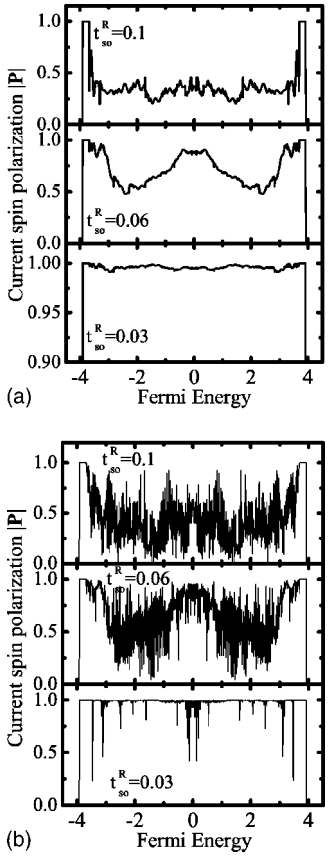

FIG. 3. Purity of transported spin states through a clean semiconductor nanowire 10×100 with different strengths of the Rashba SO coupling $t^R_{\rm SO}$. The case (a) should be contrasted with Fig. 2 where the only difference is the number of transverse propagating modes (i.e., channels) in the leads through which electrons can be injected. In (b), a tunnel barrier has been introduced between the lead and the 2DEG wire by reducing the strength of the lead-2DEG hopping parameter from $t_{L\text{-Sm}}=t_o$ in case (a) to $t_{L\text{-Sm}}=0.1t_o$ in plot (b).

entangled with the "environment" composed of two open orbital conducting channels of the same electron

$$|\text{out}\rangle = a|\nearrow\rangle\otimes|e_1\rangle + b|\swarrow\rangle\otimes|e_2\rangle. \tag{20}$$

The scattering at the lead-semiconductor interface, which in the presence of the SO interaction give rise to the nonseparable (or entangled) state in Eq. (20), is generated by the different nature of electron states in the wire and in the leads.

Recent studies have pointed out that interface between an ideal lead (with no SO couplings) and a region with strong Rashba SO interaction can substantially modify spin-resolved conductances[42] and suppress spin injection.[55] Furthermore, here we unearth how moderate SO couplings (the values achieved in recent experiments are of the order of[62] $t^R_{\rm SO}\sim0.01$) in wires of a few nanometers width will affect the coherence of ballistically transported spins, even when utilizing wires with Rashba=Dresselhaus SO couplings[18] (see also Fig. 8 below). This effect becomes increasingly detrimental when more channels are opened, as demonstrated in Fig. 3(a) for an $M=10$ channel nanowire. Thus, such mecha-

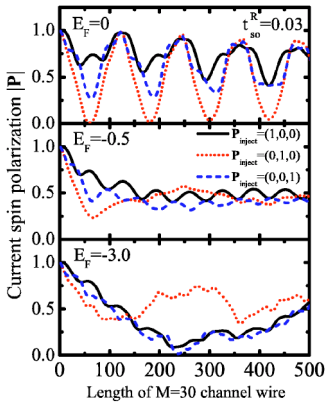

FIG. 4. (Color online) Transport of spin coherence along the ballistic nanowires of different length L. The wires are modeled on the lattice $30\times L$ with the Rashba SO interaction strength $t^R_{\mathrm{SO}}=0.03$ and the corresponding spin precession length $L_{\mathrm{SO}}=\pi t_o a/2t^R_{\mathrm{SO}}=52a$. The injected fully spin-polarized electron states from the left lead have spin ↑ pointing in different directions with respect to the Rashba electric field (Fig. 1). The number of open conducting channels is 10 at $E_F=-3.0$, 23 at $E_F=-0.5$, and 30 in the band center $E_F=0$.

nism of the reduction of spin coherence will affect the operation of any multichannel spin-FET,[68] independently of whether the semiconductor region is clean or disordered. Note also that injection through both channels of the two-channel wire is not equivalent to transport with only the first two channels opened in the $M=10$ channel wire case because unoccupied modes can influence the transport through open channels in a way that depends on the shape of the transverse confinement potential.[69]

Since tunnel barriers have become an important ingredient in attempts to evade the spin injection impediments at the FM-Sm interface,[6] we introduce the tunnel barrier in the same ballistic setup by decreasing the hopping parameter between the lead and the wire in Fig. 3 to $t_{L\text{-Sm}}=0.1t_o$. Although a tunnel barrier inserted into an adiabatic quantum point contact changes only the transmissivity of each channel without introducing the scattering between different channels,[66] here the scattering at the interface takes place in the presence of SO interactions. Thus, it can substantially affect the spin coherence of outgoing spins transmitted through two tunnel barriers in Fig. 3(b).

To understand the transport of spin coherence along the clean wire, we plot $|\mathbf{P}|$ in Fig. 4 as a function of the wire length. Contrary to the intuition gained from the DP mechanism, which in unbounded diffusive systems leads to an exponential decay of $|\mathbf{P}|$ to zero for any nonzero SO interaction, the spin coherence in clean wires displays oscillatory behavior along the wire or attains a residual value which exemplifies a partially coherent spin state. Similar behavior has been recently confirmed for semiclassical transport through confined disorder-free structures with integrable classical dynamics.[40] These effects depend strongly on the direction of spin of the injected electrons with respect to the Rashba electric field (Fig. 1) and on the concentration of carriers. Nevertheless, in some range of parameters apparently DP-like spin relaxation to zero can occur for short

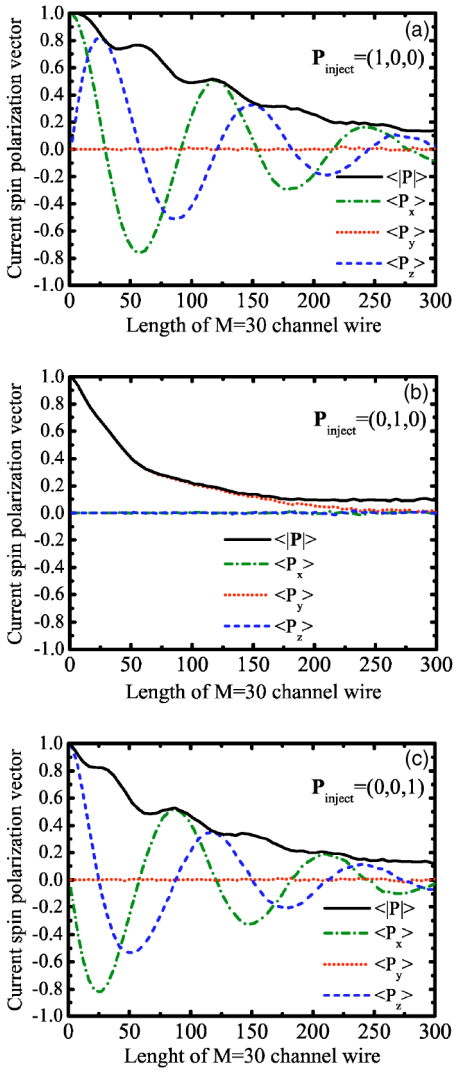

FIG. 5. (Color online) The disorder-averaged components of the spin-polarization vector $(\langle P_x\rangle_{\mathrm{dis}},\langle P_y\rangle_{\mathrm{dis}},\langle P_z\rangle_{\mathrm{dis}})$, as well as its magnitude $\langle|\mathbf{P}|\rangle_{\mathrm{dis}}$, for the outgoing current as a function of the length L of the weakly disordered semiconductor quantum wire modeled on the lattice $30\times L$ with Rashba SO interaction $t^R_{\mathrm{SO}}=0.03$ ($L_{\mathrm{SO}}=52a$) and the disorder strength $W=1$ (which sets the mean free path $\ell\simeq 4a$). The injected electrons with $E_F=-0.5$ are spin ↑ polarized along (a) the x, (b) the y, and (c) the z axis.

enough wires. This would appear as a finite spin coherence length in ballistic wires where no impurity scattering along the wire takes place.[34,40]

In the absence of external magnetic fields or magnetic impurities, the SO couplings dominate spin dynamics in semiconductor systems with inversion asymmetry due to either crystalline structure or physical configuration. In such systems, they lift the spin degeneracy of Bloch states while at the same time enforcing a particular connection between wave vector and spin through the remaining Kramers degeneracy[50] (stemming from time-reversal invariance which is not broken by the effective momentum-dependent magnetic field corresponding to SO interactions) of states $|\mathbf{k}\uparrow\rangle$ and $|-\mathbf{k}\downarrow\rangle$. For example, this leads to the applied electric field inducing spin polarization in addition to charge

current[23] or correlations between spin orientation and carrier velocity that are responsible for the intrinsic spin Hall effect.[13,70]

While coupling of spin and momentum is present in the semiclassical transport,[23,41] for quantum-coherent spatial propagation of electrons it can be, furthermore, interpreted as the *entanglement* of spinor and orbital wave function, as exemplified by the nonseparable[47] quantum state in Eq. (20). Note that this type of nonseparable quantum state describing a single particle has been encountered in some other situations[30]—for example, even when the initial state is a product of a spinor and a wave function of momentum, the state transformed by a Lorentz boost is not a direct product anymore because spin undergoes a Wigner rotation which depends on the momentum of the particle. These examples of entanglement of spin and orbital degrees of freedom (described by state vectors belonging to two different Hilbert spaces) are somewhat different from more familiar entanglement[47] between different particles, which can be widely separated and utilized for quantum communication,[30,32] because both degrees of freedom (spin and momentum) belong to the same particle. Nevertheless, their formal description proceeds in the same way—the state of the spin subsystem has to be described by a reduced density matrix obtained by tracing $|\text{out}\rangle\langle\text{out}|$ in Eq. (20) over the orbital degrees of freedom[33]

$$\hat{\rho}_s = \text{Tr}_o|\text{out}\rangle\langle\text{out}| = \begin{pmatrix} |a|^2 & ab^*\langle e_2|e_1\rangle \\ a^*b\langle e_1|e_2\rangle & |b|^2 \end{pmatrix}. \quad (21)$$

Here we utilize the fact that the type of quantum state in Eq. (20), containing only two terms, can be written down for each outgoing state in the right lead for any number of open conducting channels $\geqslant 2$. That is, such Schmidt decomposition consists of only two terms if one of the two subsystems of a bipartite quantum system is a two-level one (independently of how large is the Hilbert space of the other subsystem).[47]

The decay of the off-diagonal elements of $\hat{\rho}_s$ in Eq. (21), represented in a preferred basis $(|\uparrow\rangle,|\downarrow\rangle$ selected by the properties of incoming current), is an example of formal description of decoherence of quantum systems.[32,33] The information about the superpositions of spin-$\uparrow$ and spin-$\downarrow$ states is leaking into the "environment" (comprised of the orbital degrees of freedom of one and the same electron) while the full quantum state still remains pure as required in mesoscopic transport. It is important to clarify that the loss of coherence in the entangled transported spin state, as an exchange of phase information between the orbital and spin subsystems, occurs here without any energy exchange that often accompanies decoherence in solid state systems. Such decoherence without involvement of inelastic processes can, in fact, unfold at zero temperature with the proviso that environmental quantum state is degenerate.[71] This situation is effectively realized in quantum transport of spin through multichannel wires, where the full electron state remains a pure one $\in \mathcal{H}_o \otimes \mathcal{H}_s$ (inelastic processes would inevitably decohere this full state). The degeneracy of the "environment" here simply means that more than one conducting channel is open at those Fermi energies in Figs. 2 and 3 where $|\mathbf{P}|<1$. Note that even when transitions between different open channels are absent (so that individual spins remain in the same channel in which they were injected and no SO entanglement takes place), the spin-density matrix of current $\hat{\rho}_c$ can still be "dephased"[26,32] when its off-diagonal elements are reduced due to the averaging [as in Eq. (10)] over states of all electrons in the detecting lead.

B. Coupled spin-charge quantum diffusion in semiconductor nanowires with SO interactions

Although the problem of spin dynamics in diffusive SO-coupled semiconductors was attacked quite some time ago,[25] it is only recently that more involved theoretical studies of spin-density transport in a 2DEG with SO interactions have been provoked by the emerging interest in spintronics.[35,49,72,73] While standard derivations[1,4] of the DP spin relaxation[25] in semiclassical diffusive transport through bulk systems start from a density matrix which is diagonal in k space, but allows for coherences in the spin Hilbert space,[1] in this section we examine quantum corrections to this picture in finite-size SO coupled systems by analyzing the decay of the off-diagonal elements of the spin density matrix Eq. (7), which is obtained by tracing over the orbital degrees of freedom of the density matrix of pure state characterizing fully quantum-coherent propagation in mesoscopic systems.

To facilitate comparison with our treatment of coupled spin-charge quantum transport, we recall here the simple semiclassical picture explaining the origin of the DP spin relaxation mechanism.[40] For example, if an ensemble of electrons, spin polarized along the z axis, is launched from the bulk of an infinite 2DEG with Rashba SO interaction $\hat{\boldsymbol{\sigma}}\cdot\mathbf{B}_R(\mathbf{k})$ in different directions, then at time $t=0$ they start to precess around the direction of the effective magnetic field $\mathbf{B}_R(\mathbf{k})$. However, scattering off impurities and boundaries changes the direction of the electron momentum $\mathbf{k}$ and, therefore, can change drastically $\mathbf{B}_R(\mathbf{k})$. Averaging over an ensemble of classical trajectories leads to the decay of the z component of the spin-polarization vector, whose time evolution is described by

$$P_z(t) = \exp(-4t\ell/L_{\text{SO}}^2), \quad (22)$$

assuming that the spin precession length L_{SO} is much greater than the elastic mean free path $\ell = v_F\tau$. For elastic scattering time shorter than the precession frequency $\tau < 1/|\mathbf{B}_R(\mathbf{k})|$, the DP spin relaxation[25] is characterized by the relaxation rate $1/\tau_s \simeq \tau \mathbf{B}_R(\mathbf{k})$. Compared to other mechanisms of spin relaxation in semiconductors that generate instantaneous spin flips (such as Elliot-Yafe or Bir-Aronov-Pikus mechanisms),[24] the DP spin relaxation[25] is a continuous process taking place during the free flight between scattering events. Thus, within the semiclassical framework,[24] the spin diffusion coefficient determining the relaxation of an inhomogeneous spin distribution is the same as the particle diffusion coefficient. This renders the corresponding spin diffusion length $L_{\text{sdiff}} = \sqrt{\mathcal{D}\tau_s} = L_{\text{SO}}$ to be equal to the ballistic spin precession length L_{SO} and, therefore, independent of ℓ. The ratio ℓ/L controls whether the charge transport is diffusive

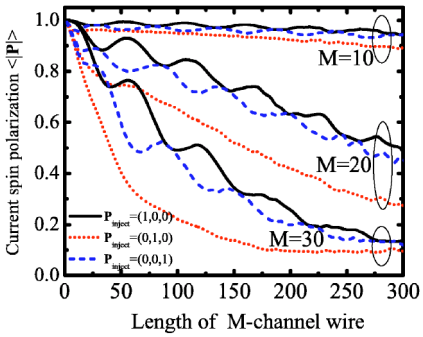

FIG. 6. (Color online) The spin polarization $\langle|\mathbf{P}|\rangle_{\mathrm{dis}}$ of current transmitted through semiconductor wires of different widths supporting different numbers of conducting channels M. The nanowires are modeled on $M\times L$ lattices where quantum transport is determined by the same set of parameters as in Fig. 5: $t_{\mathrm{SO}}^{R}=0.03$ ($L_{\mathrm{SO}}=52a$); $W=1$ ($\ell\simeq 4a$); and $E_F=-0.5$.

($\ell/L\ll 1$) or ballistic ($\ell/L\gg 1$). For a disordered 2DEG, modeled on the 2D tight-binding lattice, the semiclassical mean free path is[74] $\ell=(6\lambda_F^3E_F^2)/(\pi^3a^2W^2)$ (λ_F is the Fermi wavelength), which is valid for weak disorder $\varepsilon_{\mathbf{m}}\in[-W/2,W/2]$ in the Hamiltonian Eq. (17) and no spin-flip scattering.

To address both the fundamental issues of quantum interference corrections to spin precession and challenges in realization of semiconductor devices (such as the nonballistic mode of operation[18] of the spin-FET), we introduce the standard diagonal disorder $\varepsilon_{\mathbf{m}}\in[-W/2,W/2]$ in Hamiltonian Eq. (17) which accounts for short-range isotropic spin-independent impurity potential within the wire. The principal spin transport quantities examined in this section will be the disorder-averaged components of the polarization vector $(\langle P_x\rangle_{\mathrm{dis}},\langle P_y\rangle_{\mathrm{dis}},\langle P_z\rangle_{\mathrm{dis}})$, as well as its magnitude $\langle|\mathbf{P}|\rangle_{\mathrm{dis}}$, as a function of the wire length, disorder strength W, and SO coupling strengths. Note that in quasi-one-dimensional systems weak disorder can induce localization of electron states when their length $L\gg\xi$ becomes greater than the localization length $\xi=(4M-2)\ell$ in systems with broken spin rotation invariance.[29]

In contrast to the simple exponential decay in semiclassical theory Eq. (22), typical decay of spin polarization in the multichannel quantum wire plotted in Fig. 5 is more complicated. That is, the oscillatory behavior of $\langle P_x\rangle_{\mathrm{dis}}$, $\langle P_y\rangle_{\mathrm{dis}}$, $\langle P_z\rangle_{\mathrm{dis}}$ stems from coherent spin precession, while the reduction of $\langle|\mathbf{P}|\rangle_{\mathrm{dis}}$ quantifies spin decoherence in disordered Rashba spin-split wires. As shown in Fig. 6, the decay rate of $\langle|\mathbf{P}|\rangle_{\mathrm{dis}}$ along the wire decreases as we decrease the wire width, thereby suppressing the DP spin relaxation in narrow wires.[72] Within our quantum formalism this effect has a simple interpretation—the spin decoherence is facilitated when there are many open conducting channels to which spin can entangle in the process of spin-independent scattering that induces transitions between the transverse subbands. In all of the phenomena analyzed here, one also has to take into account the orientation of the incoming spin with respect to the Rashba electric field in Fig. 1. For example, when injected spin is polarized along the y axis, the oscillations of

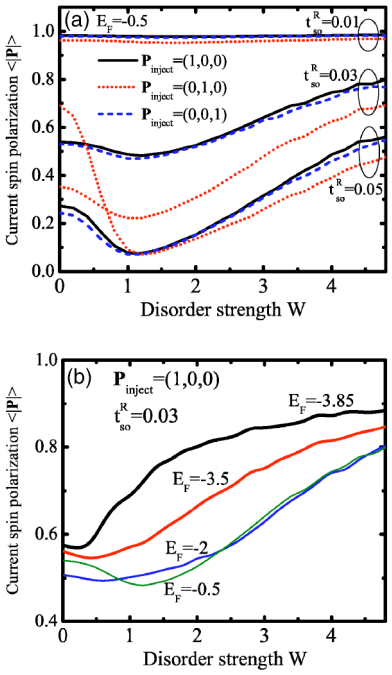

FIG. 7. (Color online) The dependence of the disorder-averaged spin polarization $\langle|\mathbf{P}|\rangle_{\mathrm{dis}}$ of the outgoing current, which has been transmitted through a semiconductor quantum wire modeled on the lattice 30×100, as a function of the disorder strength W (the corresponding semiclassical mean free path is $\ell\simeq 16at_o^2/W^2$) and the following parameters: (a) different values of Rashba coupling and direction of injected spin polarization at fixed $E_F=-0.5$; (b) different Fermi energies of transported electrons, with initial spin-↑ polarization along the x axis, in wires with $t_{\mathrm{SO}}^{R}=0.03$ ($L_{\mathrm{SO}}=52a$).

the polarization vector vanish because of the fact that $\mathbf{B}_R(\mathbf{k})$ in quasi-one-dimensional systems is nearly parallel to the direction of transverse quantization (the y axis in Fig. 1) and injected spin is, therefore, approximately an eigenstate of the Rashba Hamiltonian $\hat{\boldsymbol{\sigma}}\cdot\mathbf{B}_R(\mathbf{k})$.

There are salient features of $(\langle P_x\rangle_{\mathrm{dis}},\langle P_y\rangle_{\mathrm{dis}},\langle P_z\rangle_{\mathrm{dis}})$ in Fig. 5, brought about by SO quantum interference effects in disordered 2DEGs, which differentiate fully quantum treatment of coupled spin-charge transport from its semiclassical counterparts.[37,38] The spin polarization $\langle|\mathbf{P}|\rangle_{\mathrm{dis}}$ exhibits oscillatory behavior since spin memory is preserved between successive scattering events. As the localized regime is approached, mesoscopic fluctuations of transport quantities become as large as the average value, which is therefore no longer a representative of wire properties.[29] For the disorder-averaged polarization $\langle|\mathbf{P}|\rangle_{\mathrm{dis}}$ studied in Fig. 5, we notice that mesoscopic sample-to-sample fluctuations render it to be nonzero even after spin has traversed very long wires, i.e., $\langle\sqrt{P_x^2+P_y^2+P_z^2}\rangle_{\mathrm{dis}}\neq\sqrt{\langle P_x^2\rangle_{\mathrm{dis}}+\langle P_y^2\rangle_{\mathrm{dis}}+\langle P_z^2\rangle_{\mathrm{dis}}}$.

Fig. 7 shows how quantum interference effects in phase-coherent spin-charge transport through strongly disordered systems slow down the DP semiclassical spin relaxation,[25] while going beyond the weak localization induced slowing down[49] derived assuming weak SO coupling in random potential which can be treated perturbatively. The current spin polarization $\langle|\mathbf{P}|\rangle_{\mathrm{dis}}$ in the wires of fixed length can increase

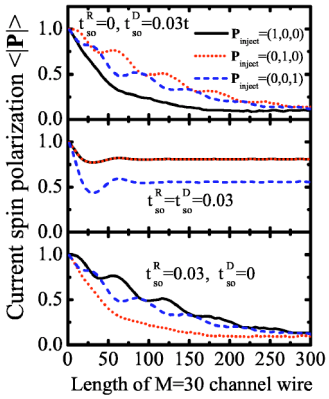

FIG. 8. (Color online) The degree of quantum coherence of transmitted spin states, measured by $\langle|\mathbf{P}|\rangle_{\mathrm{dis}}$, in a FM-Sm-FM spin-FET-like structure with disorder and Dresselhaus (top panel), Rashba (bottom panel), and Rashba=Dresselhaus (middle panel) SO couplings [as envisioned in the nonballistic spin-FET proposal (Ref. 18)]. Note that the curves for spin-↑ injection along the x and y axes overlap in the middle panel. The semiconductor region is modeled on the lattice $30\times L$ with disorder $W=1$ ($\ell\simeq 4a$) and $E_F=-0.5$ for transported electrons.

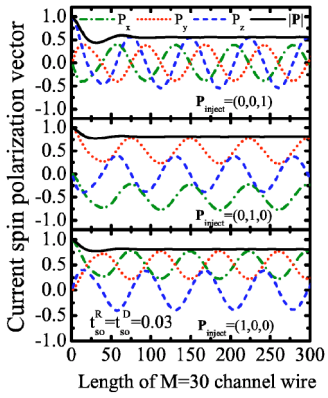

FIG. 9. (Color online) The components of the spin-polarization vector of *partially coherent* spin states that are transmitted through a nonballistic spin-FET-like structure (Ref. 18) with $t^R_{\mathrm{SO}}=t^D_{\mathrm{SO}}$. The structure is modeled by the same Hamiltonian used to compute the disorder-averaged purity of these states $\langle|\mathbf{P}|\rangle_{\mathrm{dis}}$ in the middle panel of Fig. 8.

with disorder even within the semiclassical regime $\ell > a$. This effect survives strong Rashba interaction Fig. 7 (a) or opening of more channels Fig. 7 (b). A conventional perturbative interpretation of this effect[44,49,72] is that quantum interference corrections to spin transport are generating longer τ_s, so that L_{sdiff} cease to be disorder independent. Our picture of spin entangled to the "environment" composed of orbital transport channels from Sec. III A sheds new light on this problem by offering a nonperturbative explanation for both the weakly and strongly localized regimes—as the disorder increases, some of the channels are effectively closed for transport thereby reducing the number of degenerate "environmental" quantum states that can entangle to spin.

Finally, we investigate the quantum-coherence properties of spin diffusing through multichannel wires with different types of SO interactions. As shown in Fig. 8, the spin diffusion in Rashba nanowires has the same properties as the diffusion in the Dresselhaus ones after one interchanges the direction of injected polarization for situations when incoming spins are oriented along the x and the y axes. This stems from the fact that the Rashba term and linear Dresselhaus terms can be transformed into each other by the unitary matrix $(\hat{\sigma}_x+\hat{\sigma}_y)/\sqrt{2}$. Therefore, the nontrivial situation arises when both of these SO interactions are present, as shown in the middle panel of Fig. 8.

In particular, when they are tuned to be equal $\alpha=\beta$, we find infinite spin coherence time and $L_{\mathrm{sdiff}}\rightarrow\infty$, as discovered in the nonballistic spin-FET proposal.[18] However, although the current spin polarization $\langle|\mathbf{P}|\rangle_{\mathrm{dis}}$ does not change along the wire, its length-independent constant value is set below 1, $\langle|\mathbf{P}|\rangle_{\mathrm{dis}}<1$ and, moreover, it is sensitive to the spin-polarization properties of injected current. Thus, the transported spin in such a 2DEG with carefully tuned SO couplings will end up in a mixed quantum state which remains partially coherent[75] with constant degree of coherence along the wire. The partial coherence of the state is reflected in the reduced oscillations (i.e., reduced "visibility" of spin interferences) of measurable properties $(P^\sigma_x,P^\sigma_y,P^\sigma_z)$ along the nanowire, as shown in Fig. 9 (for fully coherent states, where spin ↑ and spin ↓ interfere to form $a|\uparrow\rangle+b|\downarrow\rangle$, all components of the spin polarization would oscillate between +1 and −1). While such states are able to evade DP spin decoherence in propagation through diffusive systems,[18] they are partially coherent due to the fact that the value of their purity is set by the scattering events at the lead-2DEG interface. As demonstrated by Fig. 2 for ballistic wires with Rashba=Dresselhaus couplings, the spin decoherence processes at the interface (occurring before the diffusive regime is entered) cannot be suppressed by tuning $\alpha=\beta$.

IV. CONCLUSIONS

We have shown how to define and evaluate the spin-density matrix of current that is transmitted through a metal or a semiconductor where electrons are subjected to nontrivial spin-dependent interactions. This formalism treats both the dynamics of the spin-polarization vector and spatial propagation of charges to which the spins are attached in a fully quantum-coherent fashion by employing the transmission quantities of the Landauer-Büttiker scattering approach to quantum transport. Thus, it provides a unified description of the coupled spin and charge quantum transport in finite-size open mesoscopic structures, while taking into account attached external leads and different boundary conditions imposed by spin injection through them.

The knowledge of the spin-density matrix of electrons flowing through the detecting lead of a spintronic device allows us to quantify the degree of quantum coherence of transmitted spin quantum states as well as to compute the components of spin current flowing together with the charge current. The analysis of coherence properties of transported spin is essential for the understanding of limits of all-

electrical manipulation of spin via SO interactions in semiconductors. That is, despite offering engineered spin control, they can induce mechanisms that lead to the decay of spin coherence, even in perfectly clean systems, when electrons are injected through more than one conducting channel. We find that a single spin injected through a given channel of the left lead will end up in a partially coherent spin state in the right lead when transitions between different transverse subbands (due to scattering at impurities or interfaces) take place, thereby entangling the spin quantum state to the "environment" composed of different orbital transverse propagating modes. This is, therefore, a "genuine" decoherence mechanism[26,32] encoded in our spin-density matrix. In addition, even if every transmitted electron remains in the same channel through which it was injected, the off-diagonal elements of the spin-density matrix of the detected current can be reduced ("fake" decoherence[32] or "dephasing"[26]) due to the averaging over different channels in multichannel transport, i.e., because of an incomplete description carried out by the averaged density matrix[22,32] $\rho = 1/N \Sigma_{i=1}^{N} |\Sigma_i\rangle\langle\Sigma_i|$.

In general, reduction of visibility of quantum interference effects can arise because (i) different phases in different transmission channels prevent conditions for destructive or constructive interference being simultaneously satisfied (even though the spin states remain fully coherent) and/or (ii) the transmitted charge or spin is coupled to other degrees of freedom.[75] In the semiconductor nanowires with different types of SO couplings studied here, each spin is subjected to a genuine decoherence mechanism via unconventional realization of entanglement where the electron spin, viewed as a subsystem of a bipartite quantum system composed of spin and orbital degrees of freedom of a single electron, couples to open Landauer orbital conducting channels. The ensemble of such spins (which are not in pure, but rather in improperly mixed quantum states) in the right lead is then subjected to "dephasing" when performing the averaging of their properties in typical transport-based spin detection schemes. Such physical interpretation provides a unified description of the decay of spin coherence from the ballistic to the localized transport regime.

In most of the structures examined here, the off-diagonal elements of $\hat{\rho}_c$ do not decay completely to zero on some characteristic time scale. Instead, in the steady-state transport through multichannel wires with SO interaction spins will end up in a partially coherent quantum state.[75,76] The analysis of $\hat{\rho}_c$ for such states, which is characterized by $0 < |\mathbf{P}| < 1$, allows one to identify remnants of full spin interference effects, such as the oscillations of components of the spin-polarization vector shown in Fig. 9. Partially coherent states as the outcome of entanglement of the spin of a transmitted electron with the spin in a quantum dot have been found recently in experiments.[76] Here we find similar partially coherent outgoing spin states, which are, however, induced by a physical mechanism involving entanglement which is different and single particle in nature. Finally, even though current modulation through the coherent dynamics of transported spin in spin-FET (Refs. 17 and 18) and spin-interference ring devices[14–16] will be the strongest for single-channel semiconductor structures, quantum interference effects with partially coherent states could be utilized in realistic structures that are not one dimensional and not strictly ballistic.[16]

ACKNOWLEDGMENTS

We are grateful to S. T. Chui, J. Fabian, and L. P. Zârbo for valuable discussions.

[1] I. Žutić, J. Fabian, and S. Das Sarma, Rev. Mod. Phys. **76**, 323 (2004).
[2] *Spin Dependent Transport in Magnetic Nanostructures*, edited by S. Maekawa and T. Shinjo (Taylor & Francis, London, 2002).
[3] G. A. Prinz, Science **282**, 1660 (1998).
[4] D. D. Awschalom, D. Loss, and N. Samarth, *Semiconductor Spintronics and Quantum Computation* (Springer, Berlin, 2002).
[5] F. F. Jedema, A. T. Filip, and B. J. van Wees, Nature (London) **410**, 345 (2001).
[6] G. Schmidt, D. Ferrand, L. W. Molenkamp, A. T. Filip, and B. J. van Wees, Phys. Rev. B **62**, R4790 (2000); A. Fert and H. Jaffrès, *ibid.* **64**, 184420 (2001); E. I. Rashba, Physica E (Amsterdam) **20**, 189 (2004).
[7] Y. Ohno, D. K. Young, B. Beschoten, F. Matsukura, H. Ohno, and D. D. Awschalom, Nature (London) **402**, 790 (1999); R. Fiederling, M. Keim, G. Reuscher, W. Ossau, G. Schmidt, A. Waag, and L. W. Molenkamp, Nature (London) **402**, 787 (1999).
[8] J. M. Kikkawa and D. D. Awschalom, Nature (London) **397**, 139 (1999).
[9] M. J. Stevens, A. L. Smirl, R. D. R. Bhat, A. Najmaie, J. E. Sipe, and H. M. van Driel, Phys. Rev. Lett. **90**, 136603 (2003).
[10] P. R. Hammar and M. Johnson, Phys. Rev. Lett. **88**, 066806 (2002).
[11] J. A. Folk, R. M. Potok, C. M. Marcus, and V. Umansky, Science **299**, 679 (2003).
[12] S. K. Watson, R. M. Potok, C. M. Marcus, and V. Umansky, Phys. Rev. Lett. **91**, 258301 (2003).
[13] B. K. Nikolić, L. P. Zârbo, and S. Souma, cond-mat/0408693 (unpublished); S. Souma and B. K. Nikolić, Phys. Rev. Lett. **94**, 106602 (2005); L. Sheng, D. N. Sheng, and C. S. Ting, *ibid.* **94**, 016602 (2005); E. M. Hankiewicz, L. W. Molenkamp, T. Jungwirth, and J. Sinova, Phys. Rev. B **70**, 241301(R) (2004).
[14] J. Nitta, F. E. Meijer, and H. Takayanagi, Appl. Phys. Lett. **75**, 695 (1999).
[15] D. Frustaglia and K. Richter, Phys. Rev. B **69**, 235310 (2004); B. Molnár, F. M. Peeters, and P. Vasilopoulos, *ibid.* **69**, 155335 (2004).
[16] S. Souma and B. K. Nikolić, Phys. Rev. B **70**, 195346 (2004).
[17] S. Datta and B. Das, Appl. Phys. Lett. **56**, 665 (1990).
[18] J. Schliemann, J. C. Egues, and D. Loss, Phys. Rev. Lett. **90**, 146801 (2003).
[19] A. E. Popescu and R. Ionicioiu, Phys. Rev. B **69**, 245422 (2004);

P. Földi, B. Molnár, M. G. Benedict, and F. M. Peeters, *ibid.* **71**, 033309 (2005).

[20] Yu. A. Bychkov and E. I. Rashba, J. Phys. C **17**, 6039 (1984);P. Pfeffer, Phys. Rev. B **59**, 15902 (1998).

[21] J. Nitta, T. Akazaki, H. Takayanagi, and T. Enoki, Phys. Rev. Lett. **78**, 1335 (1997).

[22] D. D. Awschalom and J. M. Kikkawa, Phys. Today **52**(6), 33 (1999).

[23] R. H. Silsbee, J. Phys.: Condens. Matter **16**, R179 (2004).

[24] J. Fabian and S. Das Sarma, J. Vac. Sci. Technol. B **17**, 1708 (1999).

[25] M. I. D'yakonov and V. I. Perel', Fiz. Tverd. Tela (Leningrad) **13**, 3581 (1971) [Sov. Phys. Solid State **13**, 3023 (1972)]; Zh. Eksp. Teor. Fiz. **60**, 1954 (1971) [Sov. Phys. JETP **33**, 1053 (1971)].

[26] Although the vernacular terms decoherence, dephasing, and relaxation are often used as synonyms in spin physics, it is possible to make a distinction between them by classifying different types of physical mechanisms that generate the decay of the off-diagonal elements of a two-level system density matrix—see the discussion on p. 175 in Ref. 32.

[27] A. V. Khaetskii and Y. V. Nazarov, Phys. Rev. B **64**, 125316 (2001); I. A. Merkulov, Al. L. Efros, and M. Rosen, *ibid.* **65**, 205309 (2002); Y. G. Semenov and K. W. Kim, Phys. Rev. Lett. **92**, 026601 (2004).

[28] S. Datta, *Electronic Transport in Mesoscopic Systems* (Cambridge University Press, Cambridge, U.K., 1995).

[29] C. W. J. Beenakker, Rev. Mod. Phys. **69**, 731 (1997).

[30] A. Peres and D. R. Terno, Rev. Mod. Phys. **76**, 93 (2004).

[31] B. K. Nikolić, cond-mat/0301614 (unpublished).

[32] E. Joos, H. D. Zeh, C. Kiefer, D. Giulini, J. Kupsch, and I.-O. Stamatescu, *Decoherence and the Appearance of a Classical World in Quantum Theory*, 2nd ed. (Springer-Verlag, Heidelberg, 2003).

[33] W. Zurek, Rev. Mod. Phys. **75**, 715 (2003).

[34] B. W. Alphenaar, K. Tsukagoshi, and M. Wagner, J. Appl. Phys. **89**, 6863 (2001).

[35] A. A. Burkov, A. S. Núñez, and A. H. MacDonald, Phys. Rev. B **70**, 155308 (2004).

[36] M. Q. Wang and M. W. Wu, J. Appl. Phys. **93**, 410 (2003).

[37] S. Saikin, M. Shen, M.-C. Cheng, and V. Privman, J. Appl. Phys. **94**, 1769 (2003);Y. G. Semenov, Phys. Rev. B **67**, 115319 (2003);F. X. Bronold, A. Saxena, and D. L. Smith,Phys. Rev. B **70**, 245210 (2004).

[38] S. Pramanik, S. Bandyopadhyay, and M. Cahay, Phys. Rev. B **68**, 075313 (2003).

[39] E. G. Mishchenko and B. I. Halperin, Phys. Rev. B **68**, 045317 (2003).

[40] C.-H. Chang, A. G. Mal'shukov, and K. A. Chao, Phys. Rev. B **70**, 245309 (2004).

[41] D. Culcer, J. Sinova, N. A. Sinitsyn, T. Jungwirth, A. H. MacDonald, and Q. Niu, Phys. Rev. Lett. **93**, 046602 (2004).

[42] F. Mireles and G. Kirczenow, Phys. Rev. B **64**, 024426 (2001).

[43] G. Feve, W. D. Oliver, M. Aranzana, and Y. Yamamoto, Phys. Rev. B **66**, 155328 (2002).

[44] T. P. Pareek and P. Bruno, Phys. Rev. B **65**, 241305(R) (2002).

[45] H. X. Tang, F. G. Monzon, R. Lifshitz, M. C. Cross, and M. L. Roukes, Phys. Rev. B **61**, 4437 (2000).

[46] M. Popp, D. Frustaglia, and K. Richter, Nanotechnology **14**, 347 (2003).

[47] A. Galindo and A. Martin-Delgado, Rev. Mod. Phys. **74**, 347 (2002).

[48] R. M. Potok, J. A. Folk, C. M. Marcus, and V. Umansky, Phys. Rev. Lett. **89**, 266602 (2002).

[49] A. G. Mal'shukov, K. A. Chao, and M. Willander, Phys. Rev. Lett. **76**, 3794 (1996);I. S. Lyubinskiy and V. Yu. Kacharovskii-,Phys. Rev. B **70**, 205335 (2004).

[50] L. E. Ballentine, *Quantum Mechanics: A Modern Development* (World Scientific, Singapore, 1998).

[51] S. Washburn and R. A. Webb, Rep. Prog. Phys. **55**, 1311 (1992).

[52] R. Landauer, Z. Phys. B: Condens. Matter **68**, 217 (1987).

[53] J. B. Miller, D. M. Zumbühl, C. M. Marcus, Y. B. Lyanda- Geller, D. Goldhaber-Gordon, K. Campman, and A. C. Gossard, Phys. Rev. Lett. **90**, 076807 (2003).

[54] P. Středa and P. Šeba, Phys. Rev. Lett. **90**, 256601 (2003).

[55] M. Governale and U. Zülicke, Phys. Rev. B **66**, 073311 (2002).

[56] Our expression for the projection of the spin-polarization vector along the spin quantization axis Eq. (15), which is obtained from the current spin-density matrix derived in Eq. (10), can be contrasted with some of the plausible (but hard to justify rigorously) measures of "spin polarization" used in current literature, such as $P=(G^{\uparrow\uparrow}+G^{\downarrow\downarrow}-G^{\uparrow\downarrow}-G^{\downarrow\uparrow})/(G^{\uparrow\uparrow}+G^{\downarrow\downarrow}+G^{\uparrow\downarrow}+G^{\downarrow\uparrow})$ (Ref. 44).

[57] Y. Qi and S. Zhang, Phys. Rev. B **67**, 052407 (2003).

[58] S. Hikami, A. I. Larkin, and Y. Nagaoka, Prog. Theor. Phys. **63**, 707 (1980).

[59] S. V. Iordanskii, Yu. B. Lyanda-Geller, and G. E. Pikus, JETP Lett. **60**, 206 (1994); F. G. Pikus and G. E. Pikus, Phys. Rev. B **51**, 16928 (1995).

[60] T. Damker, H. Böttger, and V. V. Bryksin, Phys. Rev. B **69**, 205327 (2004).

[61] I. L. Aleiner and V. I. Fal'ko, Phys. Rev. Lett. **87**, 256801 (2001); J.-H. Cremers, P. W. Brouwer, and V. I. Fal'ko, Phys. Rev. B **68**, 125329 (2003).

[62] For example, the InGaAs/InAlAs heterostructure fabricated in Ref. 21 is characterized by the effective mass $m^*=0.05m_0$ (m_0 is the free-electron mass) and the width of the conduction band $\Delta=0.9$ eV, which sets $t_o=\Delta/8=0.112$ meV for the orbital hopping parameter in the lattice Hamiltonian Eq. (17) and $a \simeq 2.6$ nm for its lattice spacing. Thus, the Rashba coupling of the 2DEG formed in such heterostructures, tuned to a maximum value (Ref. 21) $\alpha=0.93\times10^{-11}$ eV m by the gate voltage, corresponds to $t_{\mathrm{SO}}^R/t_o\simeq0.016$ in our model.

[63] G. Dresselhaus, Phys. Rev. **100**, 580 (1955).

[64] S. D. Ganichev, V. V. Bel'kov, L. E. Golub, E. L. Ivchenko, P. Schneider, S. Giglberger, J. Eroms, J. De Boeck, G. Borghs, W. Wegscheider, D. Weiss, and W. Prettl, Phys. Rev. Lett. **92**, 256601 (2004).

[65] A. V. Moroz and C. H. W. Barnes, Phys. Rev. B **60**, 14272 (1999).

[66] B. K. Nikolić and P. B. Allen, J. Phys.: Condens. Matter **12**, 9629 (2000).

[67] B. J. van Wees, H. van Houten, C. W. J. Beenakker, J. G. Williamson, L. P. Kouwenhoven, D. van der Marel, and C. T. Foxon, Phys. Rev. Lett. **60**, 848 (1988).

[68] J. C. Egues, G. Burkard, and D. Loss, Appl. Phys. Lett. **82**, 2658 (2003).

[69] W. Häusler, Physica E (Amsterdam) **18**, 337 (2003).

[70] S. Murakami, N. Nagaosa, and S.-C. Zhang, Phys. Rev. B **69**, 235206 (2004); J. Sinova, D. Culcer, Q. Niu, N. A. Sinitsyn, T. Jungwirth, and A. H. MacDonald, Phys. Rev. Lett. **92**, 126603

(2004).
[71] Y. Imry, cond-mat/0202044 (unpublished); A. Ratchov, F. Faure, and F. W. J. Hekking, quant-ph/0402176 (unpublished).
[72] A. G. Mal'shukov and K. A. Chao, Phys. Rev. B **61**, R2413 (2000); A. A. Kiselev and K. W. Kim, *ibid.* **61**, 13115 (2000).
[73] J. I. Inoue, G. E. W. Bauer, and L. W. Molenkamp, Phys. Rev. B **67**, 033104 (2003).
[74] T. Ando, Phys. Rev. B **44**, 8017 (1991).
[75] Y. Gefen, in *Strongly Correlated Fermions and Bosons in Low-Dimensional Disordered Systems*, edited by I. V. Lerner, B. L. Altshuler, V. I. Fal'ko, and T. Giamarchi (Kluwer, Dodrecht, 2002).
[76] H. Aikawa, K. Kobayashi, A. Sano, S. Katsumoto, and Y. Iye, Phys. Rev. Lett. **92**, 176802 (2004).